WO_3 Deposited TiO_2 Nanotube Arrays by Thermal Evaporation Method for Effective Photocatalytic Activity

C. W. Lai and S. Sreekantan*

School of Materials and Mineral Resources Engineering,
Universiti Sains Malaysia, Engineering Campus,
14300 Nibong Tebal, Pulau Pinang, Malaysia

*Corresponding author: srimala@eng.usm.my

Abstract: *Titania (TiO_2) nanotube arrays were fabricated by anodising Ti foil in glycerol ($HOCH_2CH(OH)CH_2OH$) containing 0.7 g of ammonium fluoride (NH_4F). The crystal structure was studied by X-Ray Diffraction (XRD) analysis and the morphology was observed via Field Emission Scanning Electron Microscopy (FESEM). The average inner diameter of the TiO_2 nanotubes was 90 nm, and the length was approximately 2 μm. Tungsten (W) of various thicknesses was then thermally evaporated onto the TiO_2 nanotubes and annealed at 400°C in an O_2 atmosphere to form tungsten trioxide (WO_3). The effect of various thicknesses of W on the degradation of methyl orange (MO) was investigated. The sample with a 2.5 nm thick layer of W showed the best performance. The deposited W layer of that thickness is believed to provide a shallow trap for photo-generated e^- and h^+, inhibiting the recombination and extending the lifetime of the charge carriers. Thus, this sample resulted in high degradation of methyl orange (MO) as compared with other samples.*

Keywords: titania nanotube, tungsten trioxide, thermal evaporation, photocatalytic activity

1. INTRODUCTION

In the last few decades, TiO_2 has been studied extensively because of its excellent properties such as low cost, nontoxicity, high stability against corrosion, self-cleaning properties and strong oxidation ability.[1] Therefore, it is widely used in photocatalysis, photovoltaics, gas sensors, biological coatings and photoelectrolysis applications. Studies have indicated that for such applications, well-arrayed TiO_2 nanotubes are of great importance because of their one-dimensional (1D) nature, ease of handling and simple preparation.[1,2] Furthermore, the band gap of nanotube materials can be altered because of the quantum confinement effect.[2] Usually, a higher ratio of diameter to length of the tubes (aspect ratio) is preferred because this provides a larger surface area for photon absorption. Moreover, TiO_2 nanotubes contain free spaces in their interiors that can be filled with active materials such as chemical compounds,

enzymes, and noble metals, enabling them to be engineered to produce advanced multifunctional materials.[3]

To date, there are a number of preparation routes that have been reported to fabricate TiO_2 nanotubes. Techniques such as the sol-gel method, hydrothermal method, anodisation, metal-organic chemical vapour deposition (MOCVD) and templating have been reported.[4–8] However, there has been a growing interest in the anodisation method because of the resulting vertically oriented and highly ordered TiO_2 nanotube arrays, which is the most remarkable property of this method.[9,10] In 2008, Xiao et al. suggested that TiO_2 nanotubes with WO_3 deposited by a facile hydrothermal method exhibit higher photocatalytic activity.[16] Modification of TiO_2 nanotubes with cationic deposition is believed to enhance the photocatalytic activity by reducing the recombination of photogenerated electron-hole pairs.[11–16] Therefore, in this work, the effect of different thicknesses of W deposited by the thermal evaporation method onto TiO_2 nanotubes for effective photocatalytic activity was investigated.

2. EXPERIMENTAL

High purity (99.6% purity with 0.127 mm thickness) titanium (Ti) foils from STREM Chemicals were used in this study. Prior to anodisation, Ti foils were degreased in an ultrasonic bath containing ethanol for 30 minutes. The foils were then rinsed in deionised water and dried in a nitrogen stream. The anodisation was performed in a two-electrode configuration bath with the Ti foil as the anode and a platinum electrode as the counter electrode. The electrolyte consisted of 100 mL of glycerol with 0.7 g of NH_4F added. The anodisation voltage was kept constant at 40 V for 1 hour at room temperature (27°C). During the anodisation process, the fluorinated electrolyte was agitated using a magnetic stirrer. The as-anodised Ti foils were cleaned using distilled water and were dried in a nitrogen stream.

For the W deposited TiO_2 nanotube arrays, a thermal evaporation process was conducted using a K950X Turbo Evaporator thermal evaporator by EMITECH. The thickness varied from 2.5 nm to 10 nm. After the thermal evaporate process, the TiO_2 nanotube samples were annealed at 400°C for 4 hours in an oxygen (O_2) atmosphere. The morphological properties of the TiO_2 nanotubes were characterised using a Zeiss SUPRA 35VP field emission scanning electron microscope (FESEM) at working distances down to 1 mm and extended accelerating voltages ranging from 30 kV down to 100 V. The FESEM model was capable of energy dispersive X-ray (EDX) spectroscopy. To obtain the length of the nanotube layer, cross-sectional measurements were

carried out on mechanically bent samples. The actual length of the tubes was divided by cos 45º. The crystal phase of the TiO_2 nanotubes was studied by X-ray diffraction using a Bruker D8 powder diffractometer operating in the reflection mode with Cu Kα radiation (40 kV, 30 mA) and a diffracted beam monochromator. A step scan mode with a step size of 0.1° in the range of 20°–70° was also used. The photoluminescence spectra were recorded at room temperature using an LS 55 luminescence spectrometer (Jobin-Yvon HR).

The photocatalytic degradation studies were performed by dipping 4.0 cm^2 of Ti foil into 100 mL of 30 ppm methyl orange in a custom-made quartz glass photoreactor. A blank sample (without TiO_2) was also prepared to eliminate the effect of the light on the degradation of methyl orange. Both samples were left in the reactor for 30 minutes in a dark environment to achieve adsorption/desorption equilibrium. The samples were then photoirradiated at room temperature with a TUV 18W UV-C Germicidal light. Every hour, 5 mL of solution was withdrawn from each quartz tube to monitor the degradation of methyl orange after irradiation. The concentration of the degraded methyl orange was determined by using a UV spectrometer.

3. RESULTS AND DISCUSSION

3.1 Formation of TiO_2 Nanotube

Figure 1 shows the illustrative top view and cross-sectional FESEM image (the inset in Figure 1) of the TiO_2 nanotube arrays, which were grown by the potentiostatic anodisation of Ti foil at 40 V in glycerol for 1 hour. As shown in Figure 1, the anodised Ti had a complete porous structure with a well-aligned and smooth nanotube array. The average length of the tubes was 2 μm, and the diameter of the tubes was 90 nm. The aspect ratio (tube length / tube diameter) of these TiO_2 nanotube arrays was approximately 25. EDX was employed to investigate the quantity of the elements Ti and O in the anodised and annealed sample. From Figure 2, it can be concluded that the atomic ratio of Ti to O was 1:2, which confirms that this sample consisted of pure TiO_2 nanotubes without any impurity. The data are summarised in Table 1. The corresponding XRD pattern for this TiO_2 nanotube array is shown in Figure 3(a). Major peaks were detected at 25.37°, 35.67°, 48.21°, 54.10° and 55.26°, corresponding to the (101), (004), (200), (105) and (211) planes, which match with the reference pattern of anatase TiO_2, with an ICDD number of 00-021-1272.

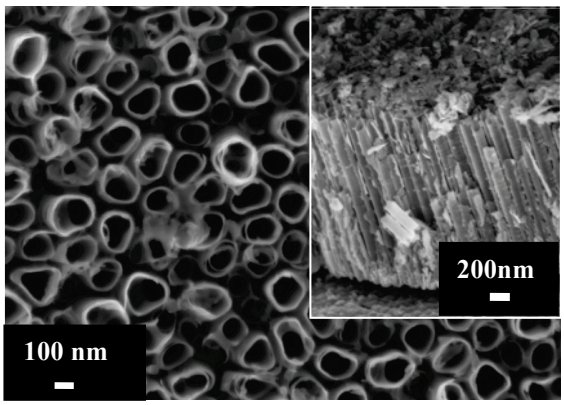

Figure 1: FESEM image of the TiO_2 nanotubes grown by anodisation in glycerol electrolyte containing 0.7 g of NH_4F.

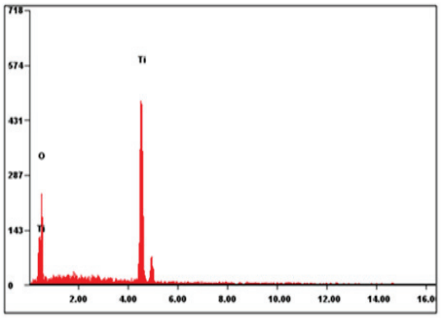

Figure 2: EDX spectra of the pure TiO_2 nanotubes.

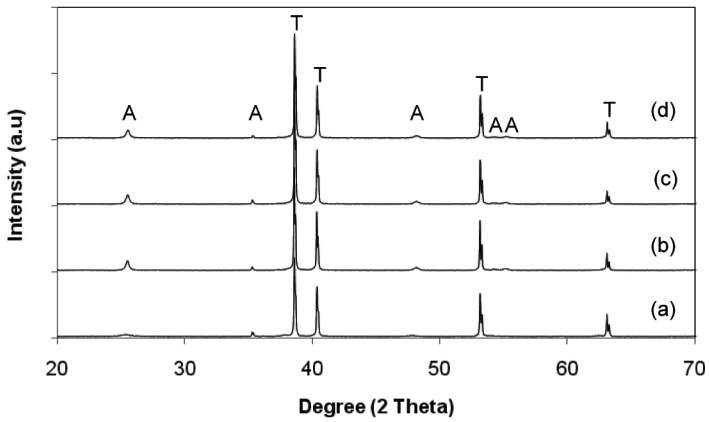

Figure 3: XRD patterns of the TiO_2 nanotubes (a) pure TiO_2 nanotubes (b) TiO_2 nanotubes deposited with 2.5 of nm W (c) TiO_2 nanotubes deposited with 5.0 nm of W (d) TiO_2 nanotubes with 10 nm of W [A= Anatase TiO_2, T=Titanium].

Table 1: Element composition for pure TiO_2 nanotubes.

Sample	Ti (wt%)	O (wt%)	W (wt%)
TiO_2 nanotube	66.66	33.34	–

3.2 Formation of WO_3 Deposited TiO_2 Nanotube

The TiO_2 nanotube arrays coated with various thickness of W were studied to evaluate the effect of W incorporation on the photocatalytic activity. Figure 4(a–c) shows the FESEM images of TiO_2 nanotubes with various thicknesses of W. A hazy, thin layer of WO_3 was found covering the wall of the TiO_2 nanotubes. The openings of the nanotubes were not covered with WO_3. EDX was performed on the thermally evaporated TiO_2 nanotube sample to determine the wt% of W incorporated on the surface of the annealed TiO_2. It can be concluded that the samples contain Ti, O and W.

The wt% of W was found to increase with the thickness of the deposited W, as shown in Figure 5. The data are summarised in Table 2. The wt% of W for 2.5 nm, 5 nm and 10 nm were 2.55, 7.07 and 13.07 wt%, respectively (Tables 2). The XRD pattern of each sample is shown in Figure 3(b–d). The majority of the peaks match those expected for the anatase phase (ICDD number 00-021-1272). Moreover, the WO_3 peak was difficult to identify in this XRD pattern; this difficulty is probably due to the amorphous nature of WO_3.

As can be seen, the intensity of the anatase peak at 25.37° corresponding to the (101) preferential orientation of the TiO_2 nanotube was enhanced after the deposition of W. This enhancement be attributed to the W atoms existing as interstitials that shared the oxygen with the Ti atoms, improving the (101) orientation of the anatase phase. This statement is in agreement with Wang et al. in 2007.[17]

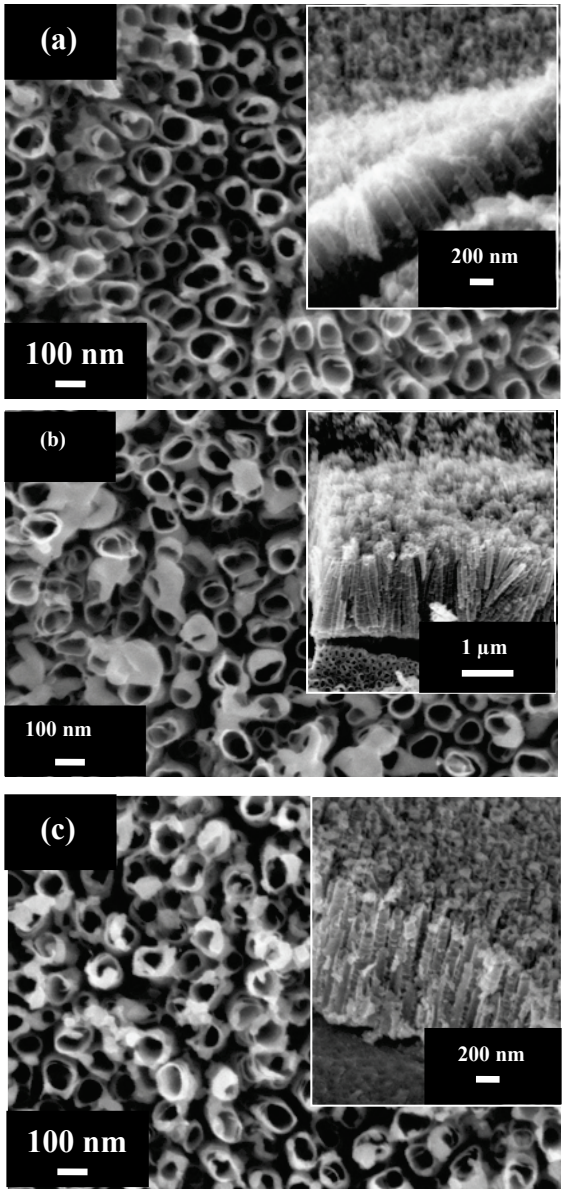

Figure 4: FESEM images of the TiO_2 nanotubes as grown by anodisation (a) deposited with 2.5 nm of W (b) deposited with 5.0 nm of W (c) deposited with 10 nm of W.

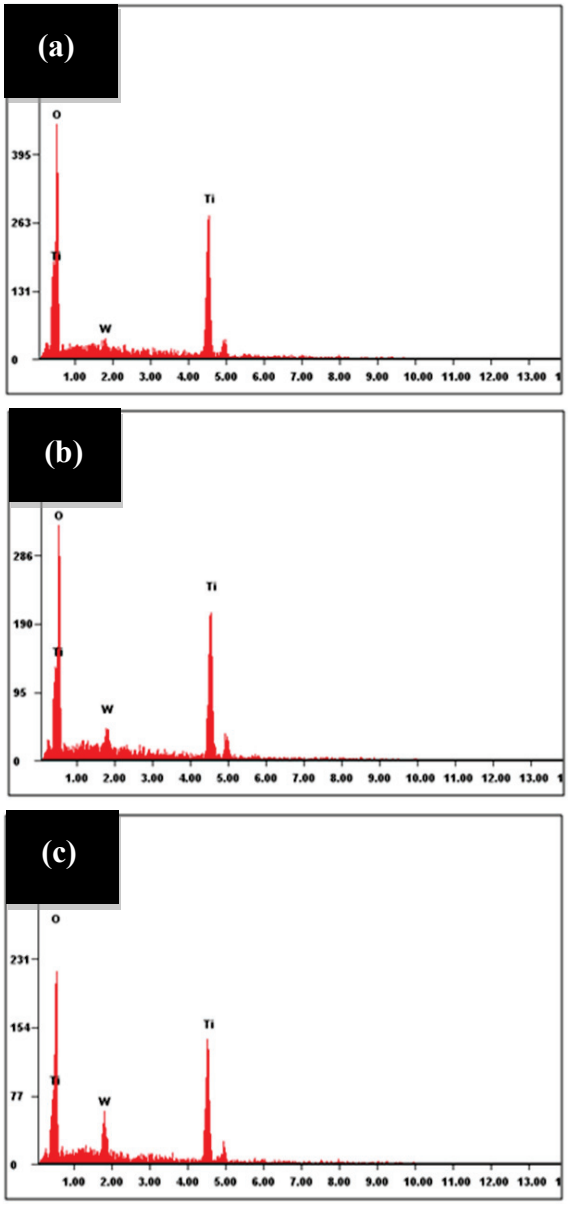

Figure 5: EDX spectra of the TiO_2 nanotubes (a) deposited with 2.5 nm of W (b) deposited with 5.0 nm of W (c) deposited with 10 nm of W.

3.3 Photoluminescence Characteristics

Photoluminescence (PL) has been used widely to investigate the energy levels of materials and to provide fundamental information on the

properties of the energy levels lying within the band gap. To study the influence of the deposited W on the luminescence of TiO_2 nanotubes, we measured the PL emission spectra of TiO_2 nanotubes deposited with different thicknesses of W in the wavelength range of 330–800 nm. The near band edge (NBE) emission at approximately 396 nm (3.2 eV) and a broad green emission centred at approximately 521 nm (2.4 eV) can be observed in the PL spectra as shown in Figure 6. These PL peaks may be closely related to the luminescence caused by the recombination of photoinduced electrons and holes, which may result from lattice distortions and surface oxygen deficiencies. The emission band centred at approximately 396 nm is assigned to the emission of a bandgap transition with photon energy approximately equal to the bandgap energy of anatase (387.5 nm). The PL signal at 521.3 nm is due to excitonic PL, which is mainly produced by oxygen vacancies. Oxygen vacancies are believed to be the main defect that causes green PL in TiO_2 nanotubes.[18,19]

Table 2: Element composition for W deposited TiO_2 nanotube.

Sample	Ti (wt%)	O (wt%)	W (wt%)
Deposited with 2.5 nm of W	63.38	34.07	2.55
Deposited with 5.0 nm of W	62.38	30.15	7.47
Deposited with 10 nm of W	55.39	31.53	13.07

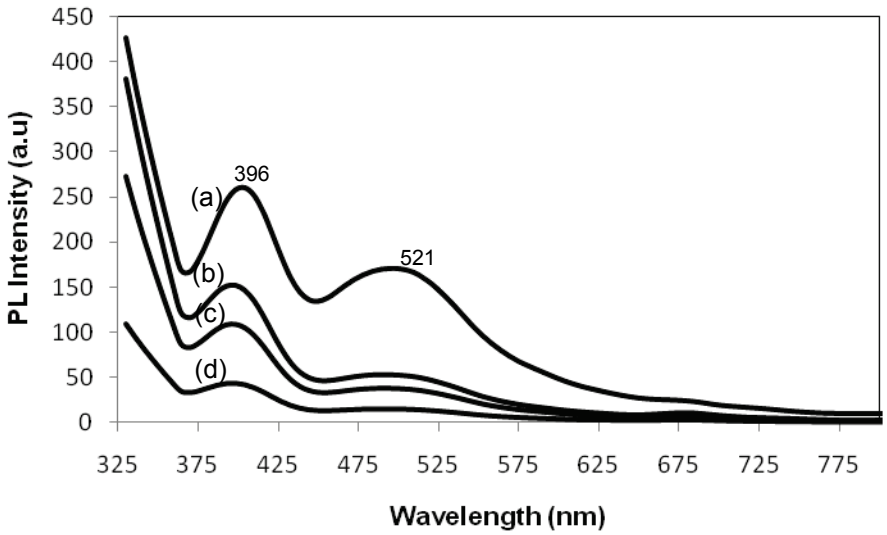

Figure 6: The PL spectra of the TiO_2 nanotubes, (a) pure TiO_2 nanotubes (b) deposited with 2.5 nm of W (c) deposited with 5.0 nm of W and (d) deposited with 10 nm of W.

Reduction in the PL intensity for the W deposited TiO_2 nanotubes compared to the pure TiO_2 nanotubes was observed. The observed PL response could be attributed to the high W content; these atoms act as the centres of electron-hole combination rather than facilitating charge transport and decreasing the rate of the radiative recombination process. The variation in PL intensity with the W content may result from the change in the defect state in the shallow level of the TiO_2 surface.[20] Furthermore, FESEM images show that the TiO_2 nanotubes are covered with WO_3 as an independent structure, which would hinder the charge transport process and act as a recombination centre.

3.4 Photocatalytic Activity

The photocatalytic activity of TiO_2 nanotubes with and without W content was evaluated by the photodegradation of methyl orange under UV light irradiation as shown in Figure 7. From the results obtained, the colour of the methyl orange (MO) changed from orange to pale orange, indicating degradation. It was noted that TiO_2 nanotubes deposited with 2.5 nm of W exhibited the highest degree of MO degradation, followed by the pure TiO_2 nanotubes and the 10 nm W deposited TiO_2 nanotubes.

The enhancement of the photocatalytic activity of the TiO_2 nanotubes deposited with 2.5 nm of thermally evaporated W was due to the coupling efficiency of the TiO_2 nanotubes and the WO_3 particles. The resulting junction between the deposited W and the TiO_2 nanotubes plays an important role in the separation of photogenerated electron-hole pairs. After the absorption of light with energy equal to or greater than the band gap, electrons and holes are generated.[15] The photogenerated electrons are transferred from the conduction band of the TiO_2 nanotubes to the conduction band of the WO_3, and the holes in the valence band of the WO_3 are transferred to that of the TiO_2 nanotubes under illumination.[16] Therefore, W deposition can provide a shallow trap for photo-generated electrons and holes, inhibiting recombination and extending the lifetime of the charge carriers. The photodegradation rate could consequently be enhanced because more charge carriers are available, and the efficiency of photocatalytic activity has been improved.[16,21]

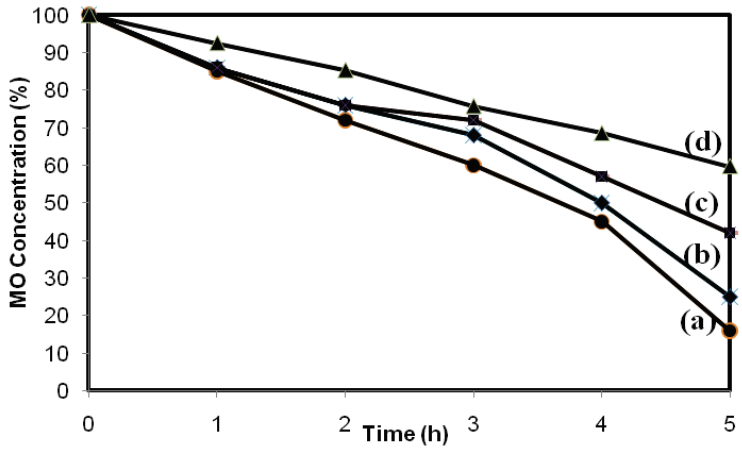

Figure 7: Degradation of methyl orange on different TiO_2 nanotube samples (a) deposited with 2.5 nm of W (b) pure TiO_2 nanotubes (c) deposited with 10 nm of W and (d) blank sample without TiO_2 nanotubes.

The poor photocatalytic activity of TiO_2 nanotubes deposited with 10 nm of W may be caused by the dilution effect of the inactive W phase.[16] The photocatalytic efficiency is decreased significantly because the inactive W phase (excess WO_3 content than optimum value in TiO_2 nanotubes) will act as the centres of electron-hole recombination easily. With thicker deposition of W, the W grows to attain independent identity, which is a distinct thin layer of WO_3 and was found covering the wall of the TiO_2 nanotubes as seen in Figure 4 (b) and (c). Most of the excited UV light is adsorbed by the thick W layer, and therefore, the transfer of electrons and holes is hindered. The photocatalytic activity decreases sharply, resulting in a level lower than that of the pure TiO_2 nanotubes. The optimum concentration can be explained by the balance of two factors: an increase in trapping sites leading to efficient trapping, and fewer trapped carriers leading to interfacial charge transfer.[15,16] Therefore, the optimum concentration of W is important to determine in order to improve the photocatalytic activity for TiO_2 nanotubes.

4. CONCLUSION

In conclusion, we report WO_3/TiO_2 nanotubes with different concentrations of W to enhance the photocatalytic activity. TiO_2 nanotubes with an average length of 2 μm and 90 nm diameter were successfully produced in a glycerol electrolyte by the anodisation method. These samples were deposited with W using the thermal evaporation technique and annealed at 400°C in an O_2 atmosphere to become WO_3. The sample with 2.55 wt% of W was found to show the most effective photocatalytic activity.

5. ACKNOWLEDGEMENT

The author would like to thank Universiti Sains Malaysia for sponsoring this work under RU grant 814075, Fellowship USM and Research University Postgraduate Research Grant Scheme, 80430146.

6. REFERENCES

1. Ni, M., Leung, M. K. H., Leung, D. Y. C. & Sumathy, K. (2007). A review and recent developments in photocatalytic water-splitting using TiO_2 for hydrogen production. *Renew. Sust. Energ. Rev.*, 11(3), 401–425.
2. Kim, S., Hwang, S. J. & Choi, W. (2005). Visible light active platinum-ion-doped TiO_2 photocatalyst. *J. Phys. Chem. B.,* 109(51), 24260–24267.
3. Sreekantan, S., Lockman, Z., Hazan, R., Tasbihi, M., Tong, L. K. & Mohamed, A. R. (2009). Influence of electrolyte pH on TiO_2 nanotube formation by Ti anodization. *J. Alloys Compd*., 485(2), 478–483.
4. Arana, J., DonaRodfquez, J. M. & Gonzalez-Diaz, O. (2004). Role of Pd and Cu in gas-phase alcohols photocatalytic degradation with doped TiO_2. *J. Photoch. Photobio. A*, 174(1), 7–14.
5. Di, L., Hajime, H., Nitin, K., Labhsetwar, K., Shunichi, H. & Naoki, O. (2005). Visible-light-driven photocatalysis on fluorine-doped TiO_2 powders by the creation of surface oxygen vacancies. *Chem. Phys. Lett.,* 401, 579–584.
6. Sobana, N., Muruganadham, M. & Swaminathan, M. (2006). Nano-Ag particles doped TiO_2 for efficient photodegradation of direct azo dyes. *J. Mol. Catal. A: Chem.*, 258(1–2), 124–132.
7. Sreekantan, S. & Lai, C. W. (2009). Study on the formation and photocatalytic activity of titanate nanotubes synthesized via hydrothermal method. *J. Alloy. Comp.,* 409(1–2), 436–442.
8. Zhu, J., Deng, Z., Chen, F., Zhang, J., Chen, H., Anpo, M., Huang, J. & Zhang, L. (2006). Hydrothermal doping method for preparation of Cr^{3+}-TiO_2 photocatalysts with concentration gradient distribution of Cr^{3+}. *Appl. Catal. B: Environ.*, 62(3–4), 329–335.
9. Anpo, M. & Takeuchi, M. (2003). The design and development of highly reactive titanium oxide photocatalysts operating under visible light irradiation. *J. Catal.*, 216(1–2), 505–516.
10. Domaradzki, J. (2003). Photoelectrical properties of heterojunction devices based on transparent oxide semiconductors on silicon. *J. Non-Cryst. Solids*, 352(23–25), 2328–2331.

11. Xiao, M. W., Wang, L. S., Huang, X. J., Wu, Y. D. & Dang, Z. (2009). Synthesis and characterization of WO_3/titanate nanotubes nanocomposite with enhanced photocatalytic properties. *J. Alloy. Compd.*, 470(1–2), 486–491.
12. Anpo, M., Takeuchi, M., Ikeue, K. & Dohshi, S. (2002). Design and development of titanium oxide photocatalysts operating under visible and UV light irradiation. The applications of metal ion-implantation techniques to semiconducting TiO_2 and Ti/ zeolite catalysts. *Curr. Opin. Solid St. M.*, 6, 381–388.
13. Idakiev, V., Yuan, Z. Y., Tabakova, T. & Su, B. L. (2005). Titanium oxide nanotubes as supports of nano-sized gold catalysts for low temperature water-gas shift reaction. *Appl. Catal. A*, 281(1–2), 149–155.
14. Kobayash, M. & Miyoshi, K. (2007). WO_3–TiO_2 monolithic catalysts for high temperature SCR of NO by NH_3: Influence of preparation method on structural and physico-chemical properties, activity and durability. *Appl. Catal. B*, 72(3–4), 253–261.
15. Wang, M., Guo, D. J. & Li, H. L. (2005). High activity of novel Pd/TiO_2 nanotube catalysts for methanol electro-oxidation. *J. Solid State Chem.*, 178(6), 1996–2000.
16. Benoit, A., Paramasivam, I., Nah, Y-C., Roy, P. & Schmuki, P. (2009). Decoration of TiO_2 nanotube layers with WO_3 nanocrystal for high-electrochromic activity. *Electrochem. Commun.*, 11(4), 728–732.
17. Wang, X. B., Song, C., Geng, K. W., Zeng, F. & Pan, F. (2007). Photoluminescence and Rahman scattering of Cu-doped ZnO films prepared by magnetron sputtering. *Appl. Surf. Sci.*, 253, 6905–6909.
18. Enache, C. S., Schoonman, J. & Krol, R. V. D. (2004). The photoresponse of iron- and carbon-doped TiO_2 (anatase) photoelectrodes. *J. Electroceram.*, 13(1–3), 177–182.
19. Knorr, F. J. C., Mercado, C. & McHale, J. L. (2008). Trap-state distributions and carrier transport in pure and mixed-phase TiO_2: Influence of contacting solvent and interphasial electron transfer. *J. Phys. Chem.*, 112(33), 12786–12794.
20. Toyoda, T., Hayakawa, T., Abe, K., Shigenari, T. & Shen, Q. (2002). Photoacoustic and photoluminescence characterization of highly porous, polycrystalline TiO_2 electrodes made by chemical synthesis. *J. Lumin.*, 87(9), 1237–1239.
21. Zhang, W. J., Li, Y., Zhu, S. L. & Wang, F. H. (2004). Copper doping in titanium oxide catalyst film prepared by dc reactive magnetron sputtering. *Catal. Tod.*, 93–95, 589–594.